

UDC 621.181.001.4:621.18

**INFLUENCE OF METAL STRUCTURAL HETEROGENEITY ON CORROSION OF STEAM BOILER PIPES**

A.S. Zavorin, L.L. Lyubimova, A.A. Makeev, A.A. Tashlykov, A.I. Artamontsev, B.V. Lebedev

Tomsk Polytechnic University

E-mail: ghost@tpu.ru

*The degree of metal structural heterogeneity and its influence on intergranular and intragranular creep and processes of general and pitting pipe corrosion of steam boilers connected with them has been estimated on the basis of the roentgenophase analysis of samples taken from pipe steel 20.*

**1. Introduction**

Corrosion processes in water-steam circuits of TES and AES are the reason of the problems of steam generator and heat-exchange pipe reliability discussed and raised periodically to the industry level [1, 2]. The developed programs of improving reliability of heat-and-power engineering equipment provide actions for upgrading chemistry conditions (CC), selecting corrosion-resistant steels and alloys and metal control as well as constructive work [3, 4]. To estimate CC at thermal and nuclear power stations the systems of chemical-engineering monitoring allowing estimating and predicting admixture behavior in water-steam circuits are developed and used; as it is known that factors of chemistry conditions as external effect factors are observed as the factors having paramount value among the reasons inducing heating surface corrosion damageability.

Corrosion metal loss for a long period in a specified medium are applied as a quantitative index of corrosion rate. However, inspite of the fact, that influence of each standard medium (water-steam, alkaline, hydrogen, oxygen, acid-phosphate etc.) is studied separately, information on corrosion rates is rather restricted even in standard media apart from practical variety of media in which heat-engineering equipment is maintained. But, on the other hand, at all variety of corrosive media the features and character of corrosive damages for them are rather uniform – local pitting damages against the background of general corrosion.

Analyzing the mechanisms of heating surface corrosive damageability the estimates of internal factor influence are presented to a less degree. Presence of phases and granules, interfaces and intergranular boundaries, structural irregularity and material heterogeneity, un-equiaxety and anisomerousity, anomalous expansions of crystal lattices etc. is referred to them [5]. A less studied field – the influence of internal residual structural voltages and their redistribution at pipe operation in conditions of temperatures and pressures on development of pitting corrosion is singled out among these problems. Exclusion of this factor from corrosion mechanism analysis deprives a complex corrosive problem of that compound approach which is required at investigations of such multiple-factor phenomenon as corrosion destruction of boiler pipe metal.

In this connection, the aim of this work is to establish a relation between internal structural voltages and corrosion rate.

**2. Experimental part****2.1. Sample preparation**

Flat samples (two sets) for corrosion tests with average sizes  $10 \times 28 \times 5$  mm were cut of boiler pipe made of steel 20, Fig. 1.

*The first set* consisted of sixteen samples each of which (excluding check test piece № 1) underwent internal mechanical load by a standard hydraulic press. The experience data [6] showed that different levels of external load influence negatively the samples. Initiating redistribution of internal voltages due to microstructural damageability they result in general decrease of sample corrosion resistance. Values of load on samples of the first set were different and amounted for different samples from 18 to 455 MPa.

*The second set* of seventeen samples underwent one and the same load equal 350 MPa. Before corrosion tests the samples were annealed on the air in the furnace at temperature about 350...400 °C.

The samples of the first and the second sets were tested for corrosion resistance in water vapor medium during the year. Every 6 months (the first and the second corrosion tests respectively) they were withdrawn from test device (Fig. 2), their mass change was determined; microhardness and internal structural voltages of the first and the second types were measured.

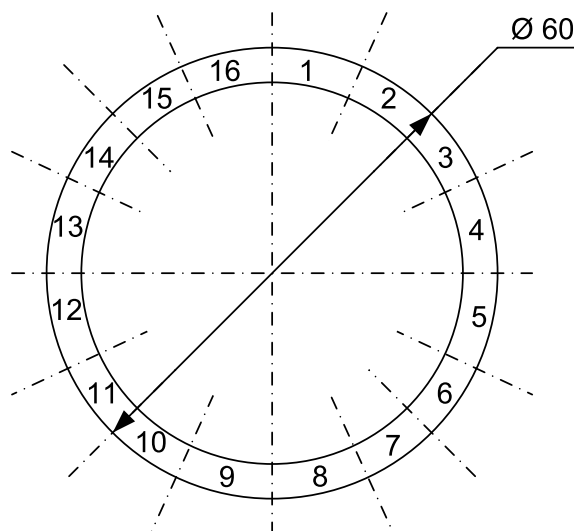


**Fig. 1.** The diagram of cutting and sample marking

2.2. The corrosion test technique

Corrosion tests were carried out in the device (Fig. 2) including work area – 1, representing a pipe of stainless steel 12X18H12T with length 500 mm, outside diameter 20 and wall thickness 2,5 mm. The work area with the studied samples was placed in the furnace – 2. The work area pipe was filled up with distilled water. Tightness was supported by argon-arc welding. Water vapor pressure in pipe cavity was measured by a standard pressure gage – 3. Temperature in work area cavity was generated by a furnace, established by a master – 4 and regulated automatically by thyristor regulator – 5 by the data of thermocouple – 6. The accurate value of temperature was read by indices of mercury thermometer – 7. The needle valve – 8 was intended for pressure release and blasting of work area cavity.

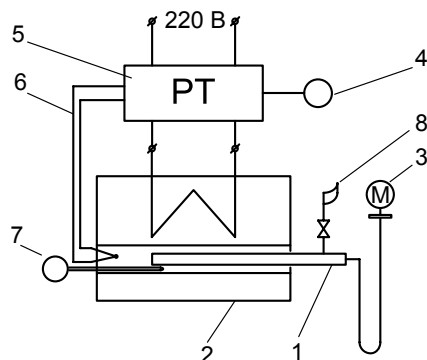
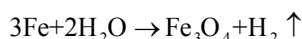


Fig. 2. The diagram of the device for corrosion tests in saturated vapor medium

Thermal conditions of the tests is steady-state (at stable temperature), around-the-clock. When being heated, water was deaerated by blasting through the needle valve. Steel was oxidized in water vapor medium by the reaction at hydrogen formation:



Hydrogen partial pressure was calculated by Dalton law:  $P_{\text{H}_2} = P_0 - P(t_s)$ , where  $P_0$  is the pressure by manometer;  $t_s$  is the saturation temperature recorded by mercury thermometer;  $P(t_s)$  is the reference value determined by tables of water and water vapor. Corrosion test temperature is 230...235 °C.

2.3. X-ray diagnostics

Internal structural voltages  $\sigma$  and crystallite sizes  $D$  are determined by the method of X-ray diffraction. For this purpose a type of functions for profiles and intensity distribution in experimental profiles of two diffraction lines for the studied sample and comparison sample are established; intrinsic physical broadening of each line for the studied sample is singled out; influence of geometrical factor is excluded; contribution into intrinsic physical broadening of each line of the analyzed sample depending on dispersion ( $m_1$  and  $m_2$ ) and on microstresses ( $n_1$  and  $n_2$ ) is estimated. After that  $D$  and  $\sigma$  are calculated by the expressions:

$$D = \frac{0,94 \lambda}{m_1 \cos \theta_1}, \quad \sigma = \left( \frac{n_2}{4 \text{tg} \theta_2} \right) \cdot E,$$

where  $\lambda$  is the wave length;  $E$  is the modulus of elongation;  $m_1$  is the part of physical broadening of the first diffraction line conditioned by crystallite sizes;  $n_2$  is the part of physical broadening of the second diffraction line conditioned by microstresses;  $\theta_1$  and  $\theta_2$  are the diffraction angles for the first and the second diffraction lines.

Dislocation density is estimated according to

$$\rho = \frac{3}{D^2}.$$

The following expressions:

$$\rho = \frac{4 \text{ctg} \theta}{5 b^2} \beta^2 \text{ and } \rho = \frac{3 \delta}{D b},$$

in which  $b$  is the strength of dislocations;  $\beta$  is the broadening of diffraction line (in radians) are used for approximate calculation of an average angle of block disorientation  $\delta$  [7]

3. The results

Two series of corrosion tests for each sample set were carried out by the developed technique for checking out the hypothesis on connection of pipe steel corrosive behavior with internal voltage distribution.

The results of the test are given in Fig. 3–6 and in the Tables 1, 2. Changes of internal voltages of the second kind  $\sigma_{II}$  for the original samples of the first and the second sets, samples after deformation by pressure, after the first and second corrosion tests depending on structural defect density are shown in Fig. 3 and 5. Sample mass change at two stages of corrosion tests are shown in Fig. 4 and 6.

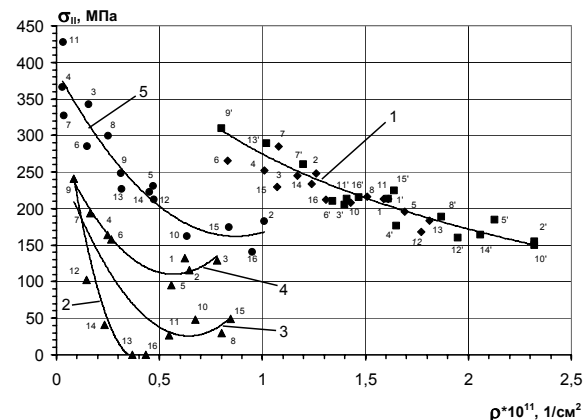
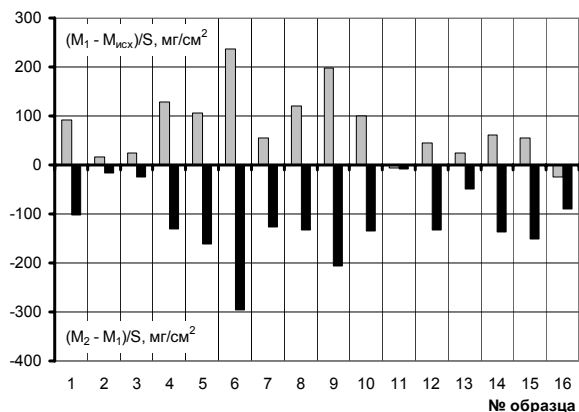


Fig. 3. Dependence of microstresses of the second type on dislocation density for the first set of samples: 1) original samples and after plastic deformation (◆, ■); 2–4) after the first corrosion tests (▲); 5) after the second corrosion tests (●)

The results of sample corrosion tests show the following.

1. Dependences of internal voltages on structural defect density for all original samples and samples of the first set after plastic deformation as well as samples of the second set after mechanical load (Fig. 3,

curve 1, and Fig. 5) are similar to Oding basic curve [8], characterizing metal resistance to plastic deformation depending on dislocation density [8].



**Fig. 4.** Change in metal mass of the first sample set: ■ –  $(M_1 - M_{исх})/S$  are the first corrosion tests; ■ –  $(M_2 - M_1)/S$  are the second corrosion tests;  $M_{исх}$  is the original sample mass;  $M_1$  and  $M_2$  are the masses after the first and the second corrosion tests;  $S$  is the sample area

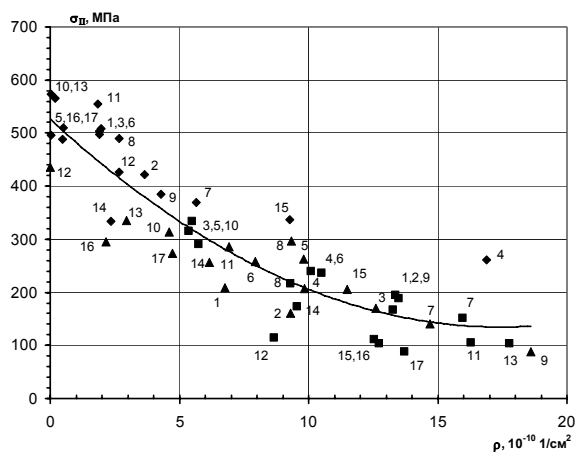


**Fig. 5.** Dependence of second type microstresses on dislocation density for the second set of samples: ◆ – original samples; ■ – after the first and ▲ – the second corrosion tests

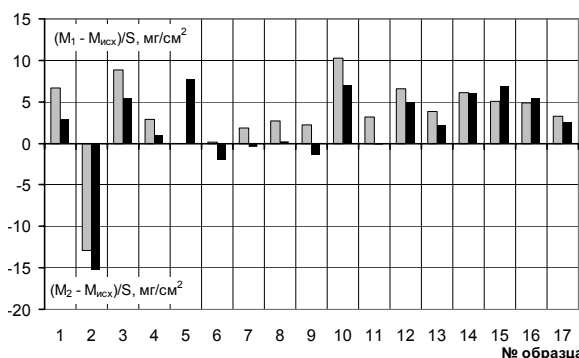


**Fig. 6.** Change in metal mass of the second sample set: ■ –  $(M_1 - M_{исх})/S$  are the first corrosion tests; ■ –  $(M_2 - M_{исх})/S$  are the second corrosion tests. See notations in Fig. 4

2. The first stage of corrosion tests of the first sample set is accompanied by overweight for all samples ex-

cluding the sample № 16 which was damaged before tests by voltage exceeding ultimate strength to destruction  $\sigma_b$  applied to it. This sample was characterized by constant metal loss without passivation during the first and the second corrosion tests.

**Table 1.** Average angle of block disorientation (the first sample set),  $\delta$ , degree

№ of a sample	Original samples	Original samples after pressure deformation	After the first corrosion tests	After the second corrosion tests
1	0,205	–	0,128	0,147
2	0,200	0,218	0,124	0,167
3	0,194	0,193	0,137	0,155
4	0,189	0,196	0,106	0,142
5	0,204	0,219	0,112	0,147
6	0,182	0,192	0,106	0,135
7	0,200	0,200	0,106	0,130
8	0,202	0,209	0,115	0,151
9	0,241	0,195	0,111	0,140
10	0,196	0,216	0,109	0,137
11	0,205	0,196	0,095	0,137
12	0,200	0,200	0,074	0,142
13	0,200	0,200	0,076	0,133
14	0,194	0,210	0,067	0,143
15	0,185	0,210	0,121	0,155
16	0,191	0,200	0,082	0,151

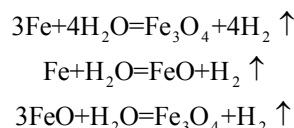
Note: the first sample did not undergo pressure deformation.

**Table 2.** Average angle of block disorientation (the second sample set),  $\delta$ , degree

№ of a sample	Original samples after pressure deformation	After the first corrosion tests	After the second corrosion tests
1	0,124	0,187	0,155
2	0,203	0,179	0,155
3	0,201	0,187	0,176
4	0,224	0,184	0,173
5	0,196	0,180	0,190
6	0,213	0,185	0,178
7	0,200	0,187	0,178
8	0,217	0,173	0,198
9	0,196	0,186	0,183
10	0,200	0,175	0,174
11	0,200	0,176	0,181
12	0,196	0,139	0,139
13	0,207	0,182	0,167
14	0,226	0,163	0,166
15	0,212	0,160	0,181
16	0,174	0,158	0,146
17	0,187	0,160	0,161

Note: the seventeenth sample did not undergo pressure deformation,  $\delta = 0,187$  degree represents the original value of an average angle of block disorientation.

3. Corrosion rate estimated by overweight is explained by metal consumption for formation of heavy oxide  $Fe_3O_4$  film in water vapor medium without oxygen:



Formation of magnetite  $\text{Fe}_3\text{O}_4$  on sample surface is confirmed by X-ray analysis of corrosion products.

4. It follows from the diagram of mass change of the first set samples after the first corrosion tests (Fig. 4) that all samples are divided into three groups: samples № 6 and 9 refer to the first one with the highest overweight 200...230 mg/cm<sup>2</sup>; samples №№ 2, 3, 11, 13 make the second group with the least overweight – from 8 to 50 mg/cm<sup>2</sup>. The rest samples referred to the third group takes the intermediate place. It is sample № 1 (check test piece which did not undergo pressure) and samples №№ 4, 5, 7, 8, 10, 12, 14, 15, which are characterized by mass increase to 150 mg/cm<sup>2</sup>.
5. The curves of changing sample internal voltages from dislocation densities after the first corrosion tests (Fig. 3, curves 2–4) show: a) departure of all experimental points from the basic curve 1; b) decrease of dislocation density of all samples due to crystallite  $D$  growth, i.e. recrystallization at low temperatures; c) internal voltage relaxation as a particular creep case, whence it follows that one must take this phenomenon into account at low test temperatures 230 °C.
6. At the second stage of the corrosion tests of the first sample set  $\text{Fe}_3\text{O}_4$  is dissolved and metal mass decreases at resumption of thin layers of  $\text{Fe}_3\text{O}_4$  oxide. Metal corrosion with mass loss occurs faster than passivation. In this case, mass change character at the second stage of corrosion tests remains: those samples which gained mass slower lose the least of mass; these are samples №№ 2, 3, 11, 13; samples № 6 and 9 lose the most of mass. Maximal mass loss amounts to 200...300 mg/cm<sup>2</sup>. The rest of samples take the intermediate position.
7. The second stage of corrosive tests is characterized by increase of internal voltages due to the creep which is considered as a periodically occurring process of strengthening-softening (Fig. 3, curve 5).
8. All stages of corrosion tests are described by different curves «voltage-dislocation density»; the return of points to the initial basic curve 1 is not observed (Fig. 3), that indicates the qualitative change of physical properties of pipe steel samples as the obtained similar curves [8] characterizes in each point a real metal strength.
9. For the samples of the second set (Fig. 5) undergone preliminary thermal treatment by annealing, the initial basic curve of internal voltage dependence on dislocation density remains approximately during all tests.
10. The corrosion rate of the second sample set (Fig. 6) is expressed in a slight mass increase (excluding sample № 2) during both the first and the second corrosion tests. Overweight does not exceed 10 mg/cm<sup>2</sup> that in 20...30 times lower than the corrosion rate in comparison with the first sample set.
11. The data on change of average angle of block disorientation given in Tables 1, 2 show that the range of these changes for the first sample set after the first

corrosion tests amounts from 3 to 9 min after the second corrosion tests – from 1 to 5 min. The angle changes from 0,6 to 4 min for the samples of the second set after the first corrosion tests and after the second corrosion tests – from 0 to 2 min.

#### 4. The results discussion

Plastic deformation, by the data of different authors, occurs by a number of mechanisms (11 mechanisms) which may be subdivided into three groups: a) a group of shearing processes – normal shift; twinning as a plastic deformation caused by shearing processes; bending; plates formation; b) a group of diffusion process – diffusion plasticity, solution-precipitating mechanism, dislocation-diffusion mechanism; c) a group of border processes – grain relative movement, block relative movement, polygonization, recrystallization [8].

Plastic deformation for one and the same metal may occur by more than one of these mechanisms; at simultaneous action of a number of mechanisms at possible predominance of one or another or several mechanisms.

Plastic deformations occur at service of pipe surface of steam boiler heating and determine such processes important for their resource as creep and relaxation of voltages.

At present the most significant standard mechanism conditioning creeping is the formation, movement and interaction of dislocation as well as diffusion processes although the obtained empirical equations of complex creeping curves with unsteady creep rates at all curve sections derived on the basis of dislocation and diffusion processes do not disclose the nature of this phenomenon and correspond to the test data only on limited sections.

Structural creep theory includes also dislocation theory, consisting in the fact that there is a number of imperfections – dislocations in crystal lattice, as the main statement; their movement causes plastic deformation under the action of external forces. Plastic deformation resistance (yield stress) is determined by shear modulus  $G$ ; this value change at temperature change determines the efficiency of creep and relaxation, for example, the higher shear modulus the higher heat resistance.

There is a critical stress value of dislocation shift  $\tau_{kp}$ , which is not determined, nevertheless, only by  $G$ , Burgers vector  $b$  and length of generating dislocation source  $l$ , as dislocation movement is complicated by a number of obstacles.

Vacancies, dislocated atoms, atoms included into solid solution are referred to such obstacles; increasing density of these «point» obstacles amplifying resistance to dislocation movement and plastic deformation. Temperature fluctuations and diffusion processes release dislocation from these obstacles. The most stable obstacles are the zonal ones – Guinier-Preston zones and fine-dispersed crystal formations; that is owing to the structural creep theory, the heterogeneous alloys resist most of all to creep. Another type of obstacles is a

«cloud» of strange atoms; it is a volume obstacle capable of dislocation steady blocking. Besides, another dislocations being not in parallel planes but crossing the glide plane may be an obstacle for dislocation movement. Dislocation as an obstacle is sensitive to temperature factor especially, at low deformation rates, i.e. in creep conditions.

Metal destruction character at creeping may be intergranular, intragranular and mixed [8] that was firstly indicated by Baili. He noted that metal behavior at creeping is determined by two factors – 1) grain ultimate strain; 2) ultimate strength of grain boundaries.

At present the part of intergranular and intragranular creeping is significant in steel heat resistance. The results of investigations of this plasticity type role come to the fact that creeping picture is qualitatively similar with plastic deformation features at active tension.

It is shown in [8] that intergranular plasticity is: 1) a method of relative movement of grains; 2) a method of recrystallization when grain size has considerably grown due to dislocation movement on grain boundaries.

These data indicate the fact that grain growth is observed at temperatures lower in comparison with general recrystallization temperature.

Therefore, intergranular plasticity at creeping may be discovered through the group of border processes [8] – relative grain or block movement and recrystallization owing to grain boundary migration detected in the given work.

In [8] the shift lines inside a grain could not be observed with the help of usual optical microscope. So, the question occurred whether plastic deformation takes place in grains.

The supposition on the fact that both intergranular plasticity which may be diagnosed by processes of boundaries recrystallization and migration and intragranular creep may be determined by crystal growth at decrease of structural defect density is put forward in this work.

In particular, crystal growth and decrease of dislocation density of the first sample set after the first corrosion tests (Fig. 3) indicate recrystallization processes inside a grain and presence of intragranular plasticity.

Curves for samples of the second set both after the first and after the second corrosion tests (Fig. 5) possess high stability; all points are in the range of basic curve,

diagnostic character of intergranular and intragranular corrosion plasticity appear to a less degree, so one can expect sufficient stability and corrosive behavior.

## 5. Conclusion

The existing ideas on presence of two types of strength – grain strength and strength of intergranular boundaries – are involved in this work for interpretation of the obtained experimental results.

It is shown that the creep phenomena may occur in steels without external active load; dislocations may move under the influence of residual inhomogeneous internal stresses.

It was ascertained that the samples without preliminary thermal treatment experience at corrosion the relaxation of internal voltages and creep of two types – intergranular and intragranular. The first one occurs radiographically in change of angles of block disorientation and the last one is accompanied by recrystallization processes inside a grain. Deformations accumulated during the tests result in strengthening of these samples at the second stage of corrosion tests. It is shown that recrystallization processes occur during corrosion tests at temperatures rather lower than usual ones. This fact ascertained that the processes of boiler pipe creep should be taken into account not at temperatures higher than 450 °C, as is customary, but at any temperatures at all stages of maintenance.

It is supposed that the presence of two types of creep results in intergranular and intragranular transformation and two types of corrosion damages – general corrosion and structural pitting corrosion.

At preliminary thermal sample treatment the thinnest solid kish occurs on their surface and in microcracks formed at plastic deformation. This kish serves as a barrier for dislocation movement increasing critical shift stress.

Therefore, thermal treatment by annealing is of great importance as a mean of decreasing general corrosion rate and reducing the development of structural pitting corrosion due to inhibition of intergranular and intragranular creep. The character of internal stress redistribution may serve as a base for predicting pipe steel corrosion behavior.

## REFERENCES

1. Concept of RAO «EES of Russia» of technical and economic-organizing policy in the field of direct heating cogeneration and district heating / A.P. Bersenev, V.A. Malafeev, G.G. Olkhovskiy et al. – Moscow: VTI, 1997. – 44 p.
2. Savchenko V.A. Some conceptual questions of controlling lifetime of Russian AES power units // Teploenergetika. – 2000. – № 5. – P. 2–8.
3. Akolzin P.A. Corrosion and protection of metal of heat-and-power engineering equipment. – Moscow: Energoizdat, 1982. – 304 p.
4. Antikain P.A. Metals and strength calculations of boilers and pipelines. – The 4<sup>th</sup> issue. – Moscow: Energoservis, 2001. – 440 p.
5. Gerasimov V.V., Monakhov A.S. Materials of nuclear power engineering. – Moscow: Atomizdat, 1973. – 336 p.
6. Pochuev V.F. Testing the pipes of industrial and heating boilers for determining efficiency applying X-ray method: Author's abstract of dissertation ... of a candidate of technical science: 05.14.04 / Tomsk Polytechnic University. – Tomsk, 2004. – 16 p.
7. Metal science and thermal treatment of steel: 3 Volumes reference book / Ed. by M.L. Bernshtein, A.G. Rikhshtadt. – The 4<sup>th</sup> issue, revised and enlarged. V. 1. Testing methods and investigations. In 2 books. B. 1. – Moscow: Metallurgiya, 1991. – 304 p.
8. Oding I.A., Ivanova V.S., Burdukskiy V.V., Geminov V.I. Theory of creep and metal long-term strength. – Moscow: Gos. Nauchn.-techn. Izd-vo po Chernoi i Tsvetnoi Metallurgii, 1959. – 487 p.

Received on 20.12.2006